Symmetry and structure of rotating H 3 +

I. N. Kozin, R. M. Roberts, and J. Tennyson

Citation: The Journal of Chemical Physics **111**, 140 (1999); doi: 10.1063/1.479260
View online: http://dx.doi.org/10.1063/1.479260
View Table of Contents: http://scitation.aip.org/content/aip/journal/jcp/111/1?ver=pdfcov
Published by the AIP Publishing

Symmetry and structure of rotating H_3^+

I. N. Kozin[a] and R. M. Roberts
Mathematics Institute, University of Warwick, Coventry CV4 7AL, United Kingdom

J. Tennyson
Department of Physics and Astronomy, University College London, London WC1E 6BT, United Kingdom

(Received 22 February 1999; accepted 9 April 1999)

We present a global study of how the *relative equilibria* of the H_3^+ ion change as the angular momentum J increases. A relative equilibrium is a classical trajectory for which the molecule rotates about a stationary axis without changing its shape. The study confirms previous results which show that the geometry of the minimum energy relative equilibria changes from an equilateral triangle to a symmetric linear configuration at around $J=47$. The series of bifurcations and stability changes that accompany this transition is presented in detail. New results include the discovery that the rotating equilateral triangle remains linearly stable for a large range of angular momentum values beyond the point where it ceases to be a minimum of the total energy. A third type of relative equilibrium, a rotating isosceles triangle, is also found to be linearly stable in the approximate range $J=0-34$. Both the equilateral and isosceles triangle configurations lose stability via Hamiltonian–Hopf bifurcations. The frequencies and symmetry species of the normal modes of the stable relative equilibria are computed and harmonic quantization is used to predict how the symmetries of the lowest lying quantum states will change as J increases. Energy level clustering due to tunneling between symmetry-equivalent relative equilibria is described. © *1999 American Institute of Physics.* [S0021-9606(99)02325-9]

I. INTRODUCTION

Relative equilibria (RE) of molecules are classical trajectories corresponding to steady rotations about stationary axes during which the shape of the molecule remains constant. Although RE are an inherently classical concept, their behavior has direct implications for the analogous quantum system. The main idea is to use the fact that the total angular momentum **J** is an integral of motion and the Hamiltonian can be regarded as parameterized by $J=|\mathbf{J}|$. For each J the Hamiltonian has a certain number of RE. In our analysis the RE play the same basic role as absolute equilibria in the traditional approach.[1] The difference is that RE are functions of J and are usually multiple due to the presence of symmetry in the Hamiltonian. The total energy of a RE may include a very high rotational contribution, resulting in a strong perturbation for which the conventional ro-vibrational theory is no longer valid. This paper presents developments of previous work by Zhilinskii, Pavlichenkov, and Kozin,[2,3] and Roberts, Sousa Dias, and Montaldi[4] on bifurcations of RE in molecules.

The method is aimed principally at the explanation and prediction of qualitative features in quantum spectra. It is expected that stable RE organize regions of phase space in which the classical dynamics are predominantly regular and will have regular spectral patterns associated with them. Changes of stability and bifurcations of RE must, therefore, affect the structure of the quantum energy levels. The structural rearrangement of rotational levels in the spectra of H_2X-type molecules was predicted in this way in Ref. 2. High values of the total angular momentum were considered in Ref. 3, but they were essentially kept to below the dissociation energy, partly due to the lack of potential functions which are accurate at higher energies. However, the method itself has no such limitation and for this paper we set out with the more ambitious aim of obtaining a complete global picture of all the RE of a triatomic molecule and how they vary with J. The result is the RE *bifurcation diagram* shown below as Figs. 2 and 4.

To illustrate the method we have chosen to study the H_3^+ ion as it is extremely light and very high rotational excitations can be obtained experimentally by electric discharge. We were motivated by the pre-dissociation spectra observed by Carrington and his group in the energy range 870–1090 cm^{-1}.[5] The spectrum corresponding to dissociation products with low kinetic energy consists of thousands of lines. A review of theoretical progress in explaining this has been given by Pollak and Schlier.[6] According to them the low kinetic energy release spectrum corresponds to transitions between ro-vibrational metastable states above the dissociation energy with moderate values of the total angular momentum (up to about 10). There has been less investigation of high kinetic energy release spectra but energy releases of over 3500 cm^{-1} have been observed.[8] These spectra display a sparser structure than those for low energy release. It has been argued[6] that the tunnelling occurs close to the top of a rotational barrier to dissociation and the translational energy can be estimated as the zero energy of H_2 subtracted from the difference between the barrier and dissociation energies. This suggests that energy release of 3500 cm^{-1} should cor-

[a]Permanent address: Institute of Applied Physics, Uljanov St. 46, 603600 Nizhnii Novgorod, Russia. Electronic mail: kozin@maths.warwick.ac.uk

respond to J values of around 45–50 [see Fig. 4 below and Fig. 1(c) (Ref. 7)].

We use the Born–Oppenheimer potential energy function for H_3^+ due to Dinelli, Polyansky, and Tennyson (DPT).[9] This has been fitted directly to the experimental data which it reproduces to near experimental accuracy. The DPT potential does not capture the correct asymptotic behavior since, for example, it does not distinguish between the two dissociation paths $H_3^+ \rightarrow H_2 + H^+$ and $H_3^+ \rightarrow H_2^+ + H$. The necessary corrections, incorporating the effects of interactions between the lowest lying electronic states, have been given by Prosmiti, Polyansky, and Tennyson using switching functions.[10] In our analysis we use the original DPT potential because its analytic form is simpler and to eliminate discussion of behavior near avoided crossings of electronic states. We are, therefore, assuming that the ground electronic state of the ion is isolated and our results may need to be modified for more asymptotically correct potentials. However, we will show that much of the interesting behavior occurs for potential energies well below dissociation, where these problems are not likely to be so relevant.

Rotational barriers to dissociation can confine molecules even above the dissociation energy.[11] They have successfully been applied to explain isotope effects in the photodissociation dynamics of H_3^+.[12] Furthermore, Pollak[11] showed that the geometry of the RE which minimize the energy changes from equilateral triangle to symmetric linear in the region $J = 45-50$. Our bifurcation diagram given below in Figs. 4 and 5 confirms and extends this work.

The approach described here resembles in many respects the works of Lohr on argon clusters.[13,14] It also lies behind the general formalism of Jellinek and Li[15] for the separation of rotational energy, and in particular their analysis of J-dependent normal vibrational modes. Miller and Wales[16] also classify RE (there called stationary points) by Hessian indices, but the latter are different from the ones used here. A unifying theme of all these methods is their use of the so-called effective potential function which incorporates both the potential and rotational energy and drives the molecular dynamics in the vicinity of the RE.

The ideas described here are complementary to the studies of very high vibrational excitations which seek to relate them to stable classical periodic orbits. Examples include the works on periodic orbits assignment for highly excited spectra of H_3^+[17] and the bifurcation analysis of periodic trajectories of the water molecule[18] and acetylene.[19] Both types of study are necessary to obtain a full understanding of global rotational–vibrational dynamics. As a first step the J-dependant normal mode analysis in this paper could be used to predict the existence of a wide variety of ''nonlinear normal modes,''[20] some of which will be continuations to $J>0$ of purely vibrational periodic trajectories.[7,21,22]

Another approach to the study of qualitative changes in quantum spectra uses rotational energy surfaces[23] derived as the classical limits of quantum Hamiltonians restricted to particular quantum vibrational states. Bifurcations of classical trajectories on these rotational energy surfaces can be related directly to changes in the quantum spectra.[24–26] It has been shown that it is possible to derive rotational energy surfaces directly from the total ro-vibrational Hamiltonian.[27,28] However the use of rotational energy surfaces is limited to regimes where the adiabatic separation of rotational motion can be assumed. In the present study we go beyond these limits and in particular are able to consider nonlinear and linear geometries on an equal footing.

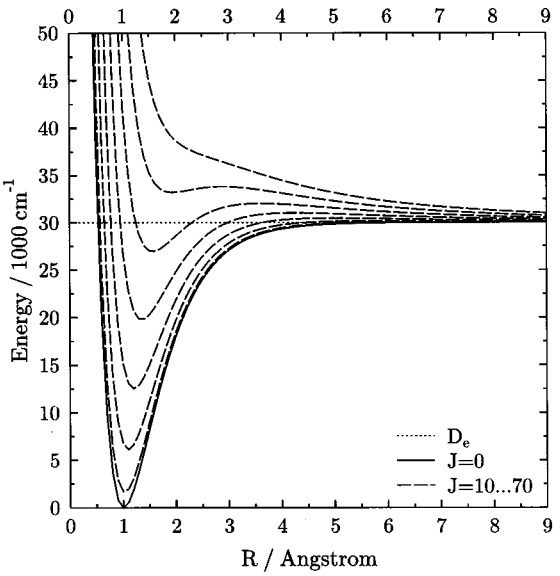

FIG. 1. The effective potential of a diatomic molecule at different values of the total angular momentum J. The dotted line shows the dissociation energy.

II. METHOD

We begin by illustrating some of the main ideas in the simple case of a diatomic molecule. This problem is effectively one dimensional because it can be reduced to the analysis of oscillations in the effective potential $V_{\text{eff}} = V(R) + J(J+1)/(2\mu R^2)$. Figure 1 shows this potential, with $V(R)$ a Morse-type function, for several different values of J. This picture should be familiar but we will work instead with the bifurcation diagram given in Fig. 2. This shows the energies of all the stationary points (maxima and minima) of the effective potential for all J. These correspond to classical trajectories in which the two particles orbit their common center of mass while maintaining the same distance apart, and are examples of RE. At low J values the effective potential has one stable stationary point (minimum) and one unstable (maximum). These two lines, depicted as solid and dashed, respectively, merge at a cusp where the two RE annihilate in an elementary bifurcation. Beyond this point there are no bound classical trajectories and no discrete quantum mechanical spectrum. The quantum energy levels in the effective potential well can also be estimated by calculating the (J-dependent) normal mode frequency of the minimum, i.e., the frequency of small amplitude oscillations about the stable RE. For this simple example no new insights are gained by considering the bifurcation diagram. However, triatomic molecules have essentially four degrees of freedom and the bifurcation diagram provides a convenient way to represent the behavior of the RE.

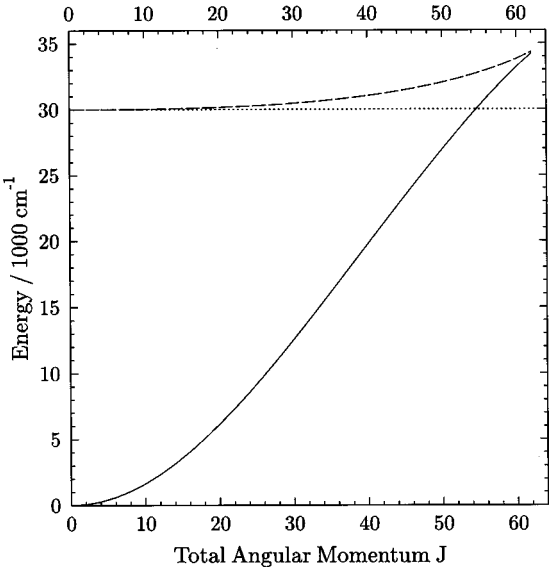

FIG. 2. The energies of RE of the effective potential $V_{\rm eff}$ (Fig. 1) as a function of the total angular momentum J. The solid line shows stable RE, the dashed line unstable RE, and the dotted line the dissociation energy.

The derivation of classical rotation–vibrational Hamiltonians can be found elsewhere;[1,3,29] in standard form it is usually written

$$H=\tfrac{1}{2}\mathbf{pdp}+\tfrac{1}{2}(\mathbf{J}-\boldsymbol{\pi})\boldsymbol{\mu}(\mathbf{J}-\boldsymbol{\pi})+V(\mathbf{q}), \tag{1}$$

where **p** is the vector of momenta corresponding to the internal coordinates **q**, **d** is the vibrational kinetic energy matrix, $\boldsymbol{\pi}$ is the vibrational angular momentum, **J** is the total angular momentum in molecule fixed coordinates, $\boldsymbol{\mu}$ is the inverted inertia tensor modified by the Coriolis terms, and $V(\mathbf{q})$ is the potential energy function expressed in the internal coordinates **q**. The Hamiltonian used here for a nonlinear triatomic molecule is the one given in Ref. 3. The shape of the molecule is described by two bond lengths and one bond angle. This choice does not make use of the full symmetry of H_3^+ but it has the advantage that it is simple and consistent with the coordinates used for H_2D^+ and D_2H^+.[29] The axis system attached to the molecule is shown in Fig. 3 and defined so that the z axis is perpendicular to the molecular plane and the y axis is parallel to the bisector of the chosen bond angle.[30] We denote the three internal coordinates by $r_1=q_1$, $\alpha=q_2$, and $r_3=q_3$.

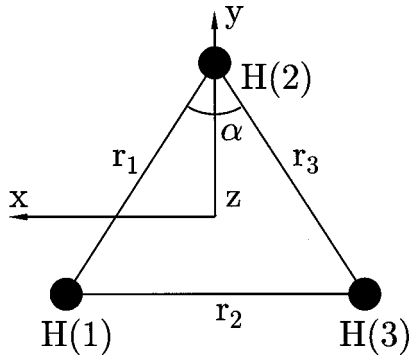

FIG. 3. The (righthand) axis system used for H_3^+. The y axis is chosen to be parallel to the bisector of the bending angle α. The z axis is perpendicular to the plane of the molecule.

Because the inertia tensor is no longer invertible the Hamiltonians (1) break down at linear configurations. There we use an alternative form which looks similar to Eq. (1) except for dimensions: The **q** and **p** vectors have dimension four while $\boldsymbol{\mu}$ is the 2×2 matrix given by

$$\boldsymbol{\mu}^{-1}=\begin{pmatrix} I'_{yy} & I'_{yz} \\ I'_{yz} & I'_{zz} \end{pmatrix}, \tag{2}$$

where $I'_{\alpha\beta}$ are the matrix elements of inertia tensor **I** modified by Coriolis terms. The total angular momentum projection on the axis of the linear configuration does not appear in the Hamiltonian. The angular momentum parallel to this axis is equal to zero and the molecule-fixed x-projection of **J** is given by vibrational angular momentum π_x expressed in terms of the internal coordinates (cf. Ref. 31). It is desirable that the new internal coordinates are consistent with the ones used for nonlinear geometries. We assume that the linear configuration corresponds to $\alpha=180°$ (see Fig. 3), the other linear configurations being obtained through the permutation of identical nuclei. However, the bond lengths–bond angle coordinates are inappropriate for linear configuration since the third Euler angle is undetermined. This problem is resolved by introducing a new auxiliary angle φ as an additional coordinate describing the rotation of the molecule about the x axis in Fig. 3, together with a transformation to a new set of coordinates q_1, q_2, q_3, q_4.[29]

The equations of motion for both these Hamiltonians are straightforward

$$\dot{q}_n=\partial H/\partial p_n, \quad \dot{p}_n=-\partial H/\partial q_n, \quad \dot{J}_\gamma=\{J_\gamma,H\}, \tag{3}$$

where Poisson brackets are used in the last equation. For the Hamiltonian for nonlinear configurations the index n is three dimensional and γ ranges over x, y, and z. For the linear Hamiltonian n is four dimensional, γ ranges over y and z. The RE are obtained as the solutions of Eq. (3) with the left hand sides set to zero. Thus, for each direction of the total angular momentum **J** determined by $\{J_\gamma,H\}=0$, the stationary points of the effective potential

$$V_{\rm eff}=V(\mathbf{q})+\tfrac{1}{2}\mathbf{J}\mathbf{I}^{-1}\mathbf{J}, \tag{4}$$

give the configurations of the molecule which steadily rotate about the axis parallel to **J**.[29] The geometry is therefore given by three equations (in the nonlinear case) or four equations (in the linear case)

$$\frac{\partial V_{\rm eff}}{\partial q_n}=0. \tag{5}$$

The molecular geometry and the direction of the total angular momentum together determine the RE.

The total angular momentum in space coordinates is an integral of motion and so $J=|\mathbf{J}|$ does not depend on time and can be regarded as a parameter. Thus the phase space is eight dimensional and the linearization of the equations of motion at a RE can be expressed in terms of four generalized coordinates and their conjugate momenta. For nonlinear configu-

rations the fourth coordinate describes precessional motion. In these coordinates the linearized equations have the general form

$$\begin{pmatrix} \dot{\mathbf{q}} \\ \dot{\mathbf{p}} \end{pmatrix} = \begin{pmatrix} (\partial^2 H)/(\partial \mathbf{p}\partial \mathbf{q}) & (\partial^2 H)/(\partial \mathbf{p}^2) \\ -(\partial^2 H)/(\partial \mathbf{q}^2) & -(\partial^2 H)/(\partial \mathbf{q}\partial \mathbf{p}) \end{pmatrix} \begin{pmatrix} \mathbf{q} \\ \mathbf{p} \end{pmatrix}. \quad (6)$$

Diagonalizing this matrix gives the harmonic frequencies (the imaginary parts of the eigenvalues) and normal modes (eigenfunctions). The RE is said to be linearly stable if the eigenvalues are all purely imaginary. Further stability information is obtained from the eigenvalues of the Hessian matrix

$$\begin{pmatrix} (\partial^2 H)/(\partial \mathbf{q}^2) & (\partial^2 H)/(\partial \mathbf{q}\partial \mathbf{p}) \\ (\partial^2 H)/(\partial \mathbf{q}\partial \mathbf{p}) & (\partial^2 H)/(\partial \mathbf{p}^2) \end{pmatrix}. \quad (7)$$

If these are all positive then the RE is a local minimum of the Hamiltonian and must be nonlinearly (Liapounov) stable as well as linearly stable. This is also true if all the eigenvalues of the Hessian are negative and so the RE is a local maximum of the Hamiltonian. This occurs for rigid rotor Hamiltonians and Hamiltonians for rotational energy surfaces, but not for the ro-vibrational molecular Hamiltonians we are concerned with here. RE may be linearly stable without being nonlinearly stable when there is a linearly stable normal mode for which the oscillations *decrease* in energy as they grow in amplitude.[32]

In the results we present below we use an index to describe the stabilities of the RE. A stable normal mode which increases in energy is assigned the symbol ''1'' while one which decreases in energy is labeled by ''-1.'' An unstable normal mode is indicated by ''0.'' Thus a nonlinearly stable RE has the index (1111) while a linearly stable RE which has one normal mode with decreasing energy has the index (111 -1).

Simple examples of these indices are provided by the RE of a rigid rotor. This is essentially a one degree of freedom system and so there is a single normal mode for each RE. The minimum energy RE are the rotations about the principal axis with largest moment of inertia. Their normal modes describe precessional motion about this axis and the energy of these increases with amplitude. Thus this RE has stability index $+1$. The maximum energy RE are rotations about the principal axis with smallest moment of inertia. For these the nearby precessional motion decreases in energy with amplitude and so these RE have stability index -1. The remaining RE are linearly unstable and have index 0.

III. SYMMETRY

Our notation for the molecular symmetry groups of the H_3^+ Hamiltonian and its RE follows closely that of Ref. 33. In molecular coordinates the Hamiltonian of the H_3^+ ion is invariant under the permutation-inversion group $D_{3h}(M)$. The Hamiltonian is also invariant under the time-reversal operation which multiplies all momenta by -1. The total permutation-inversion-time-reversal symmetry group is useful in the classification of RE. However, when labeling quantum states the time reversal symmetry does not give any additional information since it has no effect on vibrational wave functions and its action on symmetric rotor wave functions is equivalent to the actions of permutations of identical nuclei. Thus our labeling of quantum levels will make use of the $D_{3h}(M)$ group only.

The H_3^+ ion has two types of absolute equilibria. The minimum energy geometry is an equilateral triangle. This is invariant under the full group $D_{3h}(M)$ and so there is a unique configuration of this type. Small displacements of the internal coordinates from this equilibrium generate one totally symmetric A_1' and one doubly degenerate E' irreducible representations of $D_{3h}(M)$. These are the symmetry types of the normal modes of the equilateral equilibria.

In addition the H_3^+ ion has three symmetric linear equilibrium configurations which are unstable to bending deformations and so are saddle points of the potential energy function. These equilibria are invariant under a subgroup $C_{2h}(M)$ of $D_{3h}(M)$, generated by permutation of the two outer nuclei and inversion.[34] The three equilibria are transformed into each other by the remaining permutations. The four-dimensional space of small displacement of the internal coordinates near a linear equilibrium decomposes as the direct sum of one-dimensional symmetric and asymmetric stretch spaces and a two-dimensional space of bending deformations. The representations of the group $C_{2h}(M)$ on these spaces are A_g, B_u, and A_u+B_u, respectively. Note that the double degeneracy of the bending oscillations of a linear molecule is due to the spatial symmetries, not the permutation-inversion symmetries. This can be incorporated into the molecular symmetry group by the use of ''extended molecular symmetry groups.''[33] Use of the extended groups also shows that the asymmetric stretch B_u mode can not interact with the bending B_u mode.

When J is perturbed from 0, and the molecule starts rotating, its absolute equilibria bifurcate into a number of RE.[4] They differ primarily in the orientation of the total angular momentum vector with respect to the molecule. However, the centrifugal forces also effect the shape of the molecule. For J close to 0 the symmetry groups of the bifurcating RE are subgroups of the symmetry group of the original absolute equilibrium and reflect both the shape of the molecule and the direction of the total angular momentum vector. The number of bifurcating RE of each symmetry type is equal to the number of elements of the full symmetry group, divided by the number of elements of the symmetry group of the RE.

Below we describe the different types of RE that occur for H_3^+ and their molecular symmetry groups, considered as subgroups of $D_{3h}(M)$.

A. Equilateral RE

This type of RE corresponds to an equilateral triangle (ET) configuration rotating about its out-of-plane z axis. There are two such RE, corresponding to clockwise and anticlockwise rotations. The coordinates of the second one satisfy the equations $\{r_1=r_2=r_3,\ J_z=J\}$ which are invariant under the operations of the subgroup $C_{3h}(M)$ of $D_{3h}(M)$, generated by the elements E^* and (123). Permutations which

interchange two nuclei and leave the third fixed transform the two RE into each other, as does the time-reversal operation.

The symmetry types of the vibrational normal modes of the ET RE can be obtained by restricting the representations of $D_{3h}(M)$ on the normal modes of the equilateral equilibrium to the subgroup $C_{3h}(M)$. The totally symmetric A_1' mode for the equilateral equilibrium becomes the totally symmetric A' mode. The doubly degenerate E' mode retains the label E', but as a representation of $C_{3h}(M)$ this is separable,[33] i.e., the character is the sum of two complex irreducible characters which we will denote by E_a' and E_b'. The ET RE are not invariant under time-reversal and so the corresponding doubly degenerate vibrational frequency of the equilateral equilibrium splits into two distinct frequencies.

In addition to the vibrational normal modes there is also a precessional normal mode. The symmetry type of this is given by the action of $C_{3h}(M)$ on small displacements of the angular momentum vector. Since both permutations and inversion act nontrivially the representation is of type E''. Again this is separable into the sum of an E_a'' and an E_b''. The symmetry of the precessional mode is E_b'' for $J_z=J$ and E_a'' for the negative projection.

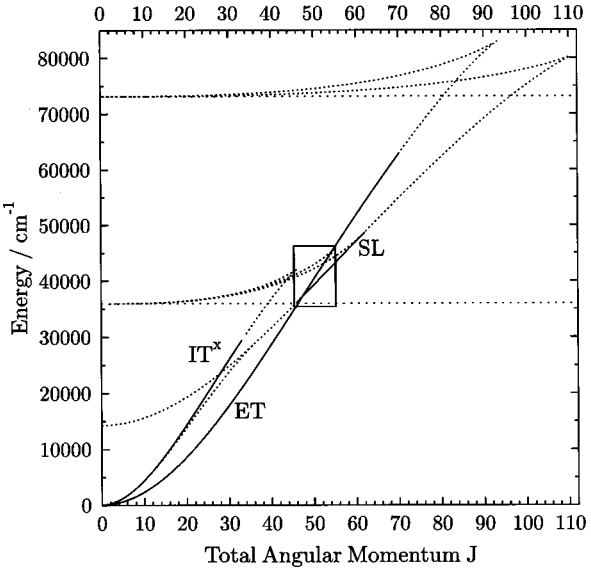

FIG. 4. The energies of the linearly stable (solid lines) and unstable (dotted lines) RE of the H_3^+ ion are shown as functions of J. Linearly stable configurations are labeled by ET for equilateral triangles, IT for isosceles triangle and SL for symmetric linear. The superscript on IT indicates the direction of the total angular momentum. The two horizontal dotted lines denote dissociation energies of the ion to two and three fragments. An enlargement of the region indicated by a rectangle is given in Fig. 5.

B. Isosceles RE

We denote a RE with the configuration of an isosceles triangle rotating about one of its principle axes by IT^{γ}, where $\gamma=x$, y, or z and denotes the axis of rotation. Representatives of each type have coordinates satisfying $\{r_1=r_3,\ J_{\gamma}=J\}$. When $\gamma=x$ this is invariant under the subgroup $C_i(M)$ of $D_{3h}(M)$ generated by $(13)^*$. The symmetry groups for $\gamma=y$ and $\gamma=z$ are $C_2(M)$ and $C_s(M)$, generated by (13) and E^*, respectively. Thus the symmetry group in each case is of order two and there are six symmetry equivalent forms for each RE.

For each of the IT^{γ} RE the symmetry types of the normal modes are determined simply by whether they are symmetric or anti-symmetric with respect to the symmetry group of the RE. In each case there are two symmetric and one anti-symmetric vibrational normal modes and the precessional normal mode is anti-symmetric.

C. Linear RE

The three symmetric linear equilibria each have molecular symmetry groups $C_{2h}(M)$, generated by a permutation of two nuclei together with inversion. The symmetric linear (SL) RE are these configurations rotating about axes which are perpendicular to the linear axes. The rotation does not break any of these symmetries, so again the molecular symmetry groups are $C_{2h}(M)$, and there are three symmetry equivalent RE. The normal modes are of the same symmetry types as for the symmetric linear equilibria, namely $A_g+A_u+2B_u$. The rotation does break the extra symmetries that appear in the extended molecular symmetry group of the symmetric linear equilibria.[34] It follows that when $J>0$ the two B_u modes can interact. Section V shows that there is indeed a mixing of asymmetric stretch modes with bending modes of the same symmetry type.

Although there are no asymmetric linear (AL) absolute equilibria for H_3^+, the corresponding RE do appear as (unstable) rotational barriers to dissociation. They have molecular symmetry groups $C_s(M)$ generated by E^* and there are six symmetry equivalent forms. Note that this is the same symmetry group as for the IT^z RE. However, they can be distinguished by the fact that time-reversal symmetry maps a linear RE to itself, while it maps an IT^z RE to a different (though still symmetry equivalent) RE.

IV. BIFURCATIONS OF RELATIVE EQUILIBRIA

Equation (5) for the RE was solved numerically using Mathematica, usually for each integer J measured in units of $\hbar$. To give a better correspondence with the analogous quantum problem J was actually taken as $\sqrt{J(J+1)}$. The DPT potential[9] was used, assuming an isolated ground electronic state. For each RE the eigenvectors of the matrix in Eq. (6) were used to transform the Hessian (7) to 2×2 block diagonal form. Then each sub-block was tested for the sign of its eigenvalues to determine the stability index defined in the previous section.

The energies of the RE were plotted as functions of J to obtain the bifurcation diagram shown in Fig. 4. The figure also includes two dissociation energies. The first one corresponds to the dissociation of H_3^+ to H_2+H^+. The dissociation to H_2^++H occurs almost 15 000 cm^{-1} higher and is not shown. The second dissociation energy in the figure corresponds to the total break-up of H_3^+ into three particles.

The solid lines in Fig. 4 represent linearly stable RE, i.e., those for which the eigenvalues of the matrix in Eq. (6) are

purely imaginary. The energies of the stable RE are labeled according to their configuration. The first impression of Fig. 4 is that it consists of a number of pairs of curves which merge at cusps. These are very similar to the pair which make up the bifurcation diagram of the diatomic molecule in Fig. 2.

At low values of J the diagram shows three curves of RE which emerge from zero and one coming from the barrier to linearity at just below 15 000 cm^{-1}. The lowest energy RE, labeled ET, correspond to steady rotations of equilateral triangle configurations about axes perpendicular to the molecular planes. At low values of J these RE are absolute minima of the energy and have stability index (1111).

Next up in energy, at low values of J, are unstable (1110) RE of type IT^y. The configuration is an isosceles triangle and the angular momentum vector points along the C_2 axis bisecting the bend angle between the two equal length bonds. Consequently, as J increases the bend angle increases, reaching 180° at a point where this family bifurcates from the SL family of RE coming from the barrier to linearity. These symmetric linear RE start off with stability index (1100) at $J=0$, but this changes to (1110) at the bifurcation point.

The six highest energy RE emerging from the origin, labeled IT^x, correspond to steady rotations of isosceles triangle configurations about axes in the molecular plane perpendicular to the C_2 axes. Initially these have stability index (111−1). The index −1 describes the stability of the precessional normal mode and means that these RE have maximum energy in the rotational energy surface model of the low J behavior. At $J\approx 34$ we observe a qualitatively new phenomenon which is absent in diatomic molecules. The IT^x RE simultaneously lose stability to two normal modes with stability indices of opposite sign, resulting in the stability index (1100). This is an example of a Hamiltonian–Hopf bifurcation.[35] At the bifurcation point the frequencies of the two normal modes become equal and the corresponding eigenvalues of the linearized equations of motion acquire real parts. See also Sec. V. Higher still in J ($J\approx 46$) the IT^x RE disappear in collisions with another family of RE of type IT^x which has stability index (1000) and which ''comes in from the dissociation limit'' as J increases from 0. This is one of the families of RE which play the same role as the rotational barriers to dissociation of diatomic molecules.

Moving up still higher in J we now turn to the bifurcations which accompany the change from equilateral triangle to symmetric linear minimum energy configurations. These can be seen most clearly in the enlargement Fig. 5. Recall that the stability of the symmetric linear RE increased from (1100) to (1110) at $J\approx$ 34, where a family of isosceles triangle RE bifurcates from it. It becomes stable, with index (1111), at a similar bifurcation at $J\approx 46$. The bifurcating RE are isosceles triangles rotating about axes perpendicular to the molecular plane and are labeled IT^z in Fig. 5. They also play a role in de-stabilizing the ET RE. As J increases the bend angle of the isosceles configuration decreases and the family of RE passes through the equilateral configuration at $J\approx 50$ in a transcritical bifurcation. At this point the stability index of ET RE changes from (1111) to (111−1) as the result of a normal mode frequency passing through 0. The IT^z RE go on to disappear in a collision with a matching rotational barrier to dissociation at $J\approx 55$. Between $J\approx 46$ and $J\approx 50$ the equilateral triangle and symmetric linear RE are both local minima of the energy, the energy of the latter dropping to below that of the former within this range. Note, however, that the energies of both types of RE are above the lowest dissociation energy, and so neither is the absolute minimum of the Hamiltonian.

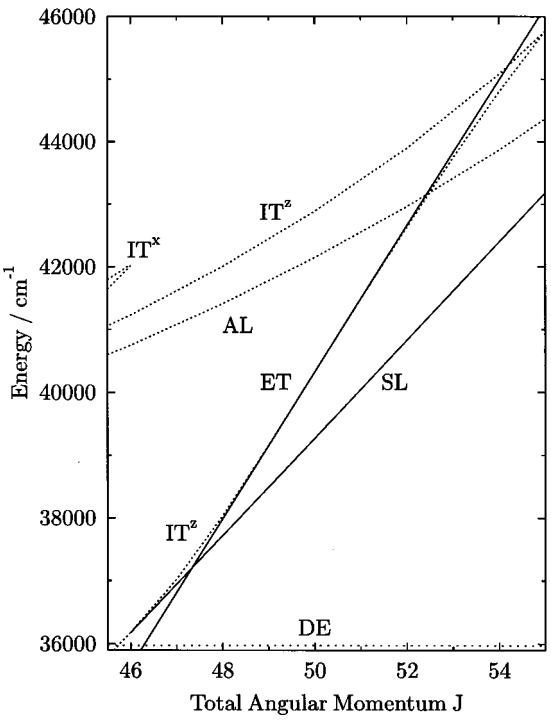

FIG. 5. An enlargement of the region indicated by the rectangle in Fig. 4. AL denotes the asymmetric linear RE. All other notation remains the same.

Returning to Fig. 4, we see that the symmetric linear RE continue to be local minimum until $J\approx 62$ where they lose stability in a bifurcation with another family of rotational barrier RE. These have asymmetric linear configurations. The equilateral triangle RE remain linearly stable until $J\approx 70$ where they lose stability in another Hamiltonian–Hopf bifurcation. Finally both these families of RE disappear in collisions with matching rotational barriers to dissociation in a similar way as for diatomic molecules.

The DPT potential[9] is expected to be increasingly poor at energies above 25 000 cm^{-1}. As a result our analysis at energies close to dissociation might only be expected to give a rough idea of what could happen. However, the energies of RE are the sums of their potential and rotational energies and frequently the latter is very large. In Fig. 6 only the potential energy is plotted and it can be seen that the bifurcations discussed in this section occur at levels where the DPT potential may still be valid even though the total energy is very high. To test the sensitivity of our results to the potential we repeated the calculations with a model pairwise potential based on just one Morse function. The resulting RE bifurcation diagram was qualitatively identical to that for the DPT potential. We believe that this is because the sequence of

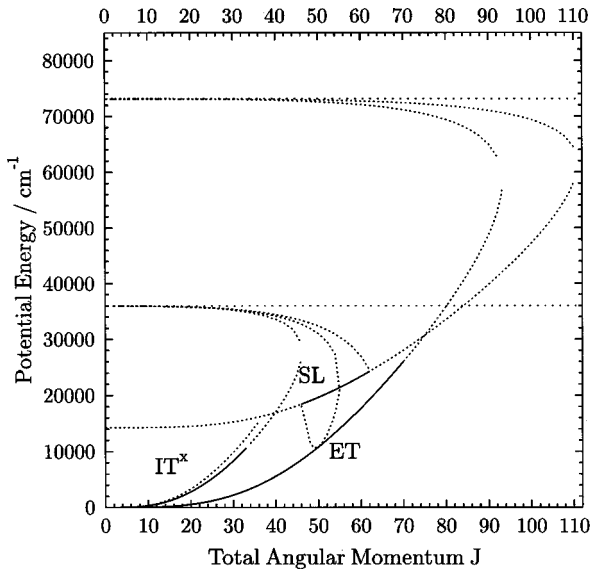

FIG. 6. The potential energy of the RE of the H_3^+ ion. The notation is the same as in Fig. 4.

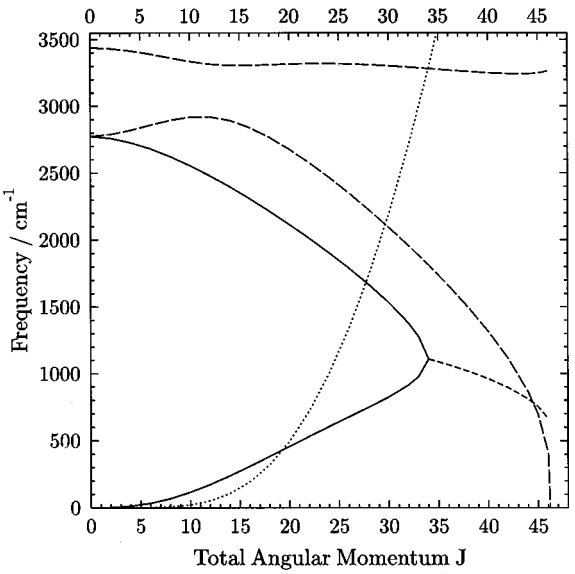

FIG. 7. Classical normal mode frequencies for the IT^x RE of the H_3^+ ion. Large dashed lines correspond to modes which are symmetric with respect to $C_i(M)$, solid lines to modes which are anti-symmetric and the small dashed line shows the real part of the complex frequency after the Hamiltonian–Hopf bifurcation at $J \approx 34$. The dotted line shows the energy difference between the IT^x and the barrier IT^y RE.

bifurcations described is the simplest way that stability can be transferred from the equilateral triangle to the symmetric linear configurations as J increases.

V. NORMAL MODES AND HARMONIC QUANTIZATION

The results of the previous section show that H_3^+ has three different types of linearly stable RE: the isosceles triangles IT^x at low values of J, the symmetric linear SL at high values and the equilateral triangles ET over a wide range of values. In this section we describe the normal modes of these RE and use harmonic quantization to make some elementary predictions about the corresponding quantum states.

The energies of quantum states which are localized near linearly stable RE can be estimated by the formula

$$E_{n_1 \cdots n_4} = E_{\mathrm{RE}}(J) + \sum_{l=1}^{4} k_l \omega_l(J)(n_l + \tfrac{1}{2}), \tag{8}$$

where $E_{\mathrm{RE}}(J)$ is the energy of the RE, n_l is the number of quanta in the lth normal mode, $\omega_l(J)$ is its frequency and k_l its stability index. This estimate ignores anharmonic corrections and also the splitting due to tunneling between symmetry equivalent RE. It will only be useful for wave functions which are localized near the RE. The minimal requirement for this is that the energy in each normal mode is lower than the tunneling barrier to another RE along that normal mode. In practice we use the criterion that half the lowest normal mode frequency is less than the energy difference between the RE and the lowest barrier.

The approximate wave functions localized near a RE can be labeled according to how they transform under the molecular symmetry group of the RE. A wave function with n_l quanta in the lth normal mode will have symmetry type

$$\Gamma^{\mathrm{loc}}_{n_1 \cdots n_4} = \Gamma_0 \otimes \Gamma_1^{n_1} \otimes \cdots \otimes \Gamma_4^{n_4}, \tag{9}$$

where Γ_0 is the symmetry of the ground state of the RE, i.e., the wave function with zero normal mode quanta, Γ_l is the representation of the symmetry group on the lth normal mode, $\otimes$ denotes the (tensor) product of representations and $\Gamma_l^{n_l}$ is the product of Γ_l with itself n_l times. The representation Γ_0 is not necessarily trivial. From the correspondence principle in the classical limit the ground state must be the symmetric top wave function $|JK=JM\rangle$, where the quantization axis is chosen along the axis of rotation of the RE.[37] The symmetry type is determined by the actions of equivalent rotations of the molecular symmetry group[33] of the RE on $|JK=JM\rangle$ and in general will vary with J.

Symmetry equivalent RE have symmetry equivalent wave functions which interact with each other via tunnelling. The resulting wave functions of the quantum states of the molecule given by harmonic approximation are linear combinations of the localized wave functions and can be labeled by how they transform under the full group $D_{3h}(M)$. The representation of $D_{3h}(M)$ on the space of all quantum states obtained in this way from a single localized wave function is the corresponding induced representation. These are most conveniently calculated using Frobenius reciprocity.[36] In general these representations are reducible and the energies of the irreducible components are split by the tunneling, giving rise to energy level clusters with characteristic symmetry properties.

A. Isosceles triangle with $J_x = J$

Figure 7 shows the normal mode frequencies for the IT^x RE. The vibrational normal modes of the $D_{3h}(M)$ equilibrium point at $J=0$ are a totally symmetric A_1' ''breathing'' mode and the doubly degenerate E' mode. For the bifurcating IT^x RE the symmetry is broken to $C_i(M)$ and the E'-mode splits into two non-degenerate vibrations which are

symmetric and anti-symmetric with respect to $C_i(M)$. The corresponding nonlinear normal modes are $J>0$ perturbations of the ''local bending'' modes.[21] The former breathing mode is also symmetric and starts to interact with the symmetric branch of the E'-mode. As J increases the centrifugal forces cause the molecule to deform into an elongated T-shape (cf. Fig. 3), the breathing mode transforms into a diatom stretching mode and the symmetric E'-mode into a dissociation mode. The frequency of the breathing/diatom mode remains roughly constant while the frequency of the dissociation mode goes to 0 at $J\approx 46$.

The frequency of the precessional mode increases from 0 as J increases. This mode is anti-symmetric with respect to $C_i(M)$ and interacts with the anti-symmetric branch of the E'-mode, resulting in a Hamiltonian-Hopf bifurcation at $J\approx 34$. Thereafter the corresponding frequencies are complex and the figure shows only their real part. Up until this point the precessional frequency is always the lowest frequency. Hamiltonian–Hopf bifurcations frequently imply the existence of monodromy in classical systems[38] and it seems likely that the corresponding quantum monodromy[39] will exist for states localized near the IT^x RE. However, this requires further investigation.

The dotted line in Fig. 7 shows the difference between the energy of the IT^x RE and that of the barrier provided by the unstable IT^y RE. The figure suggests that localized ''precessional wave functions'' should occur in the approximate range $J=15-34$. Because the precessional stability index is -1, these will decrease in energy from that of the RE as the number of quanta increases, and they will be alternately symmetric and anti-symmetric with respect to the symmetry group $C_i(M)$. The corresponding induced ''cluster representations'' of $D_{3h}(M)$ are $A_1'+E'+E''+A_2'$ and $A_1''+E''+E'+A_2''$, respectively. These representations are six dimensional, corresponding to the six symmetry equivalent IT^x RE. Tunneling will split the energy into four distinct levels, two of which are doubly degenerate.

B. Equilateral triangle with $J_z=J$

The frequencies of the normal modes for the ET RE are presented in Fig. 8. The breathing mode remains totally symmetric with respect to this group while the E'-mode, which is doubly degenerate at $J=0$, splits into E_a' and E_b'-modes as a result of the breaking of time-reversal symmetry. As J increases the frequency of the breathing mode decreases as the molecule grows in size.

In an appropriate coordinate system which preserves C_3 symmetry the nuclei in the two E'-modes undergo small oscillations around circular trajectories with their centers at the nuclear positions in the RE. The frequencies of these oscillations depend on the direction of the total angular momentum: The mode in which the nuclei circle in the same direction as the overall rotation of the molecule has lower frequency than the one for which they circle in the opposite direction. The change of stability index from (1111) to (111−1) occurs as the lower frequency passes through zero at $J\approx 50$. At this point the direction in which the nuclei circle their RE positions changes for this mode and so, for $J>50$, they oppose the overall rotation of the molecule in both E' modes. Note also that for $J>50$ the lower frequency E'-mode has less energy than the RE. At $J\approx 70$ the two frequencies collide and become complex in a Hamiltonian–Hopf bifurcation. The nonlinear normal modes associated with these normal modes are $J>0$ perturbations of the ''circular'' modes of Ref. 21.

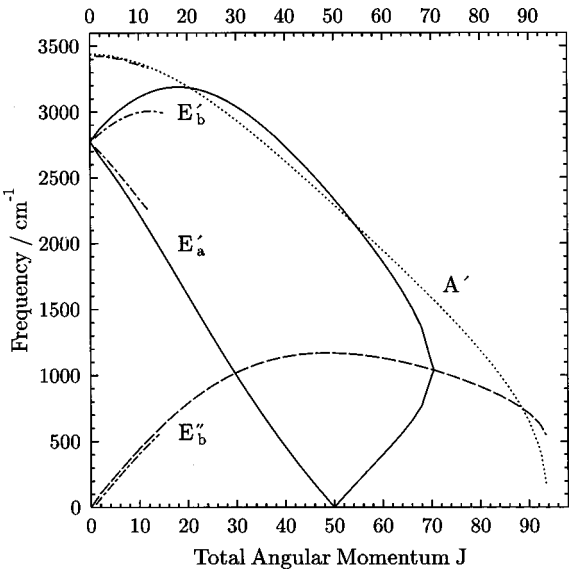

FIG. 8. Classical normal mode frequencies for the ET RE of the H_3^+ ion. The dotted line is the totally symmetric breathing mode, the solid lines are the E_a' and E_b' modes and the dashed line is the precession frequency. The dash-dot lines give the ''quantum'' estimates of the normal mode frequencies (Ref. 41).

The precession frequency grows almost linearly but then exhibits a period of stabilization. Remarkably the calculations (and Fig. 8) show that the precession frequency is equal to exactly half the difference between the two E' frequencies for $J<50$ and to half the sum of the frequencies for $J>50$. After the Hamiltonian–Hopf bifurcation the real part of the E' frequencies is equal to the precession frequency. This three way resonance is a consequence of the high degree of symmetry of the RE.

The lowest frequency normal mode is the precessional mode up to $J=30$ where it switches to being the E_a' mode until the Hamiltonian–Hopf bifurcation at $J\approx 70$. For most of this range this frequency is well below twice the height of the lowest barrier. However in the range $J=47-53$ the nearest barrier is provided by the IT^z RE and these are generally too close to those of type ET for localization to occur.

As J varies through $0\cdots 5$ mod 6, the ground state symmetry Γ_0 is A', E_a'', E_b', A'', E_a', E_b'', respectively. The local symmetry types of wave functions corresponding to excited precessional states depend on the number of quanta n mod 6. For example, suppose J is a multiple of 6 and so the ground state is totally symmetric. Then as n varies through $0\cdots 5$ mod 6, the wave functions vary through the sequence of representations: $A'\otimes(E_b'')^n=A'$, E_b'', E_a', A'', E_b', E_a''. The corresponding induced representations of $D_{3h}(M)$, and hence cluster types, are: $A_1'+A_2'$, E'', E', $A_1''+A_2''$, E', E''. This sequence, and its analogues for other values of J, agrees with the structure obtained from conventional perturbation

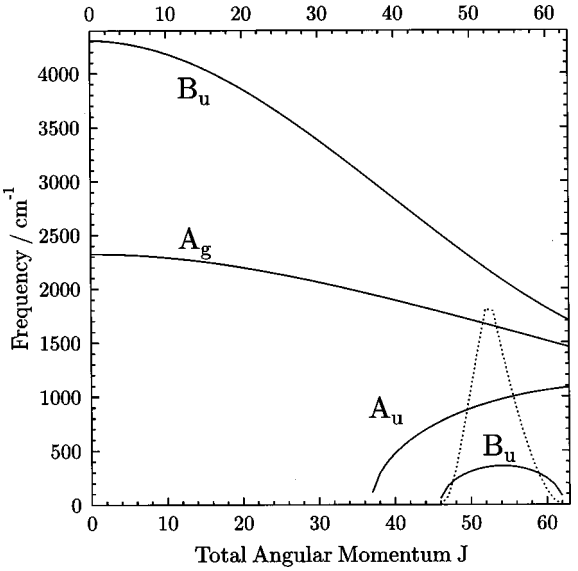

FIG. 9. The classical normal mode frequencies of the SL RE of the H_3^+ ion are shown as solid lines and labeled by the appropriate representations of $C_{2h}(M)$. The dotted line shows the energy of the barrier provided first by the IT^z RE and then the AL RE.

theory.[41,42] Similarly, for J a multiple of 6 the local symmetry types of excited E_a' wave functions depend on n mod 3 and are given by: $A' \otimes (E_a')^n = A', E_a', E_b'$ and the corresponding sequence of induced representations of $D_{3h}(M)$ is: $A_1' + A_2', E', E'$.

C. Symmetric linear

The classical normal mode frequencies of the SL RE are shown in Fig. 9. The second highest frequency mode is the symmetric stretch along the molecular axis. The highest and lowest frequency modes, both of symmetry type B_u, correspond to other oscillations in the plane perpendicular to the total angular momentum vector **J**. As J approaches 0 the highest frequency mode becomes the asymmetric stretch mode of the linear equilibrium. The lowest frequency becomes real at the bifurcation of the IT^z RE from the SL RE. It follows that at this point the corresponding normal mode is a bending vibration. However, the frequency of the same normal mode goes to 0 again at the point where the AL RE bifurcate from the SL RE. At this point the normal mode must be close to an asymmetric stretch vibration. Thus as J increases there is a complete mixing of the asymmetric stretch and bending motions perpendicular to **J**.

The remaining mode, of symmetry type A_u, corresponds to bending oscillations in the plane formed by **J** and the linear reference configuration. This mode gains stability after the bifurcation to the IT^y RE and may be thought of as a low amplitude ancestor of the rotating horseshoe periodic orbit.[7,22]

Throughout the range for which the SL RE are stable the B_u-mode which starts out as a bending oscillation perpendicular to **J** and ends up as an asymmetric stretch oscillation always has the lowest frequency. Corresponding localized wave functions should exist for J between about 48 and 59. The symmetry of the ground state wave function Γ_0 alternates between A_g (J even) and B_g (J odd). Consequently the symmetry types of excited B_u states will alternate between A_g and B_u or B_g and B_u. The corresponding cluster types will be the induced representations of $D_{3h}(M)$ obtained from these, namely $A_1' + E'$ and $A_2' + E'$ or $A_2'' + E''$ and $A_1'' + E''$, respectively.

VI. COMPARISON WITH EXPERIMENTS AND COMPUTATIONS

In principle we could express $E_{\mathrm{RE}}(J)$ and $\omega_i(J)$ as polynomial series in J^2, as has been done by Lohr and Huben[13] for $E_{\mathrm{RE}}(J)$, and compare the results with the traditional effective ro-vibrational Hamiltonian. However this is unlikely to be useful for H_3^+ because of the essentially nonpolynomial dependence of the energy on J^2. For H_3^+ effective Hamiltonians built up as power series in the total angular momentum are divergent. To overcome the problem of divergence, Padé and Borel approximations of effective Hamiltonians were suggested in Ref. 43 and used in Ref. 44. It would be interesting to test whether these approximations reproduce the energy dependence of RE given here.

Instead we evaluate how close the correspondence is between the classical and quantum mechanics by estimating the normal mode frequencies from experimental data[40] partly supplemented by quantum calculations.[45] The most straightforward comparison is for the equilateral triangle RE. The precession frequency was taken to be $E(K=J-1)-E(K=J)$ in the ground vibrational state and the vibrational frequencies were obtained by subtracting the lowest energy level for a given J-value. The result obtained was that the vibrational frequencies are uniformly higher than their estimates by $\sim 250\ \mathrm{cm}^{-1}$, presumably due to anharmonic corrections. Since our aim was to compare J-dependence we *shifted the quantum estimates* by this amount upwards. These quantum estimates of the normal mode frequencies are shown in Fig. 8 as dash–dot lines. The agreement seems to be quite satisfactory. The classical precession frequency is almost uniformly above the quantum values by $40\ \mathrm{cm}^{-1}$ which means that the relative error decreases as J grows. It is about 10% at $J=10$ and should be smaller for higher J.

Very few full quantal calculations have been performed for higher values of J, partly because of difficulties with incorporating linear geometries, and partly because of the size of Hamiltonian matrix implied by such a calculation. However, it is interesting to note that one of the very earliest *ab initio* attempts to calculate the high J spectrum of H_3^+ reported that at $J=46$ the low energy spectrum has a vibrational, rather than rotational, nature.[46] Those results are consistent with our predictions even at a numerical level. The quantum spacings between the computed doublets are about $170\ \mathrm{cm}^{-1}$ (see Table V of Ref. 46) which is very close to the frequency of $175\ \mathrm{cm}^{-1}$ we have calculated for the E_a' normal mode of the ET RE at $J=46$ (see Fig. 8). However, according to our predictions the first and second doublets of Ref. 46 must be of E' type, i.e., exactly degenerate, suggesting that there is poor convergence in the computations.

Several factors may affect the IT^x cluster formation predicted in section V A. It may be spoiled by the fact that when $J>15$ the precessional frequency is rapidly approaching that

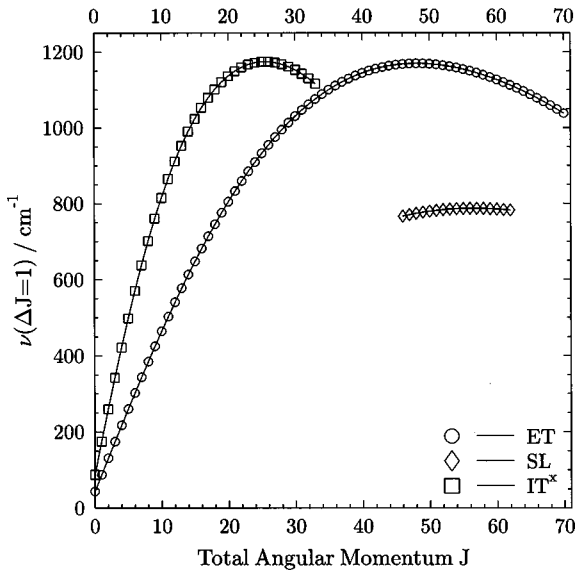

FIG. 10. Frequencies of $\Delta J=1$ transitions for all stable RE. The circles, diamonds and squares correspond, respectively, to ET, SL, and IT^x RE.

of the anti-symmetric vibrational mode. It may be facilitated by vibrational excitation since this effectively increases the barrier height. However, vibrational excitation also leads to higher level densities and more ''accidental'' resonances which may destroy the clusters. The high densities will in any case make it difficult to find the clusters.

Comparisons between any of the predictions and experimental data are complicated by the fact that due to nuclear spin statistics in H_3^+ the A_1' and A_1'' levels have zero weights[41] and so will not be seen in physical spectra. As a result only energy level triplets will be observable for the IT^x clusters and some of the energy level doublets in ET will not appear. This is not true for the analogous D_3^+ spectra for which all the levels can occur.

Some progress has been made towards understanding the pre-dissociation spectrum of H_3^+ ion.[5] Most of this spectrum was recorded at low kinetic energy release of dissociation products and it is believed that this corresponds to rather low values of J.[6] High kinetic energy release spectra should have high J values and it has been reported that they are generally more sparse.[5] If so, it is possible that regular features in these pre-dissociation spectra will correlate with transitions between levels associated with J-dependent RE as the molecules are brought to the dissociation threshold mainly through rotational excitation.

With this in mind, one can speculate about vibrational or ro-vibrational transition frequencies with the same J within particular RE using the normal frequencies given in Figs. 7–9. In Fig. 10 we present energy differences $E_{\mathrm{RE}}(J+1)-E_{\mathrm{RE}}(J)$ for all stable RE. It gives a rough idea of the pure rotational $\Delta J=1$ transition frequencies in H_3^+. Sometimes it gives perhaps just an order of magnitude, as around $J=50$ where the ET and SL RE are not well separated from each other. Sometimes it should be more reliable, as for the ET RE from $J=10-40$. All of the three bands in Fig. 10 tend to form dense groups of transitions around 1000 cm^{-1} which is close to the experimental spectral range used by Carrington and co-workers.[5,8] Intensity factors are not considered here and apparently pure rotational dipole transitions are forbidden for the equilateral configuration. But these frequencies should be regarded as the ''base'' frequencies to be supplemented by the corresponding J-dependent precession and vibrational frequencies participating in the considered transition. In harmonic approximation the ro-vibrational transition frequencies can be estimated by adding or subtracting the necessary J-dependent frequency using Eq. (8) (see Figs. 7–9). When vibrational excitation is involved, the J-dependence of the transition is likely to be pulled down since vibrational frequencies usually have negative derivatives with respect to J.

VII. CONCLUSION

In this paper we have described *all* the RE of the H_3^+ ion and how they bifurcate and change stability as J increases. The results confirm those of Refs. 11 and 22 showing that the equilateral triangle (ET) configuration is replaced as the minimum energy geometry by symmetric linear (SL) configurations at $J\approx 47$. In addition we give a detailed description of the bifurcations and stability changes that accompany this switch and shown that the symmetric linear configurations go on to lose stability at $J\approx 62$. Surprisingly, the rotating equilateral triangle remains linearly stable for a large range of J beyond the point where it ceases to be a minimum of the energy function, and indeed beyond the point where the symmetric linear configurations lose stability. We have also shown that there is a family of rotating isosceles triangle (IT^x) RE which is linearly stable in the range $J=0-34$. Both the ET and IT^x RE lose stability in Hamiltonian–Hopf bifurcations.

The normal mode frequencies for all the linearly stable RE have been computed and the results combined with harmonic quantization and symmetry techniques to make predictions about quantum states localized near the RE. The lowest energy quantum states are predicted to have the symmetry types and clustering patterns given in Sec. V. The classical analysis suggests that two main rearrangements of these levels take place as J increases. The first is associated with the precessional-to-vibrational change in the lowest frequency normal mode of the ET RE at $J\approx 30$, while the second is due to the ET to SL switch in minimum energy geometry at $J\approx 47$. The fact that the ET RE remain to be linearly stable beyond this point suggests that ''shape resonances'' associated with both symmetric linear and equilateral triangle geometry may be embedded in the continuous spectrum. Finally we have predicted that energy level quadruplets with characteristic symmetry patterns associated to the IT^x RE should occur for a range of J values starting at about $J\approx 15$. Because of spin statistics these quadruplets will be reduced to triplets in physical spectra. The possible effects of the Hamiltonian–Hopf bifurcations on these clusters, and on the quantum states associated to the ET RE, require further investigation.

ACKNOWLEDGMENTS

We are very grateful to Boris Zhilinskii for a number of very useful discussions. This work is supported by a UK

EPSRC research grant. I.N.K. thanks partial support from Russian Fund for Fundamental Research through Grant No. 97-02-16593.

[1] E. B. Wilson, Jr., J. C. Decius, and P. C. Cross, *Molecular Vibrations* (McGraw-Hill, NY, 1955).
[2] B. I. Zhilinskii and I. M. Pavlichenkov, Opt. Spectrosc. **64**, 413 (1988).
[3] I. N. Kozin and I. M. Pavlichenkov, J. Chem. Phys. **104**, 4105 (1996).
[4] R. M. Roberts and M. E. R. de Sousa Dias, Nonlinearity **10**, 1719 (1997); J. A. Montaldi and R. M. Roberts, J. Nonlinear Sci. **9**, 53 (1999).
[5] A. Carrington and R. Kennedy, J. Chem. Phys. **81**, 91 (1984).
[6] E. Pollak and C. Schlier, Acc. Chem. Res. **22**, 223 (1989).
[7] J. M. Gomez Llorente and E. Pollak, J. Chem. Phys. **90**, 5406 (1989).
[8] A. Carrington, I. R. McNab, and Y. D. West, J. Chem. Phys. **98**, 1073 (1992).
[9] B. M. Dinelli, O. L. Polyansky, and J. Tennyson, J. Chem. Phys. **103**, 10433 (1995).
[10] R. Prosmiti, O. L. Polyansky, and J. Tennyson, Chem. Phys. Lett. **273**, 107 (1997).
[11] E. Pollak, J. Chem. Phys. **86**, 1645 (1987).
[12] A. V. Chambers and M. S. Child, Mol. Phys. **65**, 1337 (1988); M. Berblinger, Ch. Schlier, and E. Pollak, J. Phys. Chem. **93**, 2319 (1989).
[13] L. L. Lohr and C. H. Huben, J. Chem. Phys. **99**, 6369 (1993).
[14] L. L. Lohr, Int. J. Quantum Chem. **57**, 707 (1996); Mol. Phys. **91**, 1097 (1997).
[15] J. Jellinek and D. H. Li, Phys. Rev. Lett. **62**, 241 (1989); Chem. Phys. Lett. **169**, 380 (1990).
[16] M. A. Miller and D. J. Wales, Mol. Phys. **89**, 533 (1996).
[17] E. Pollak, Philos. Trans. R. Soc. London, Ser. A **332**, 343 (1990).
[18] Z. Lu and M. E. Kellman, Chem. Phys. Lett. **247**, 195 (1995).
[19] R. Prosmiti and S. C. Farantos, J. Chem. Phys. **103**, 3299 (1995).
[20] J. Montaldi, M. Roberts, and I. Stewart, Philos. Trans. R. Soc. London, Ser. A **325**, 237 (1988); Nonlinearity **3**, 695 (1990); **3**, 731 (1990).
[21] D. A. Sadovskii and B. I. Zhilinskii, Phys. Rev. A **47**, 2653 (1993); D. A. Sadovskii, N. G. Fulton, J. R. Henderson, J. Tennyson, and B. I. Zhilinskii, J. Chem. Phys. **99**, 906 (1993).
[22] M. Berblinger, E. Pollak, and Ch. Schlier, J. Chem. Phys. **88**, 5643 (1988).
[23] W. G. Harter and C. W. Patterson, J. Chem. Phys. **80**, 4241 (1984); W. G. Harter, Comput. Phys. Rep. **8**, 319 (1988).
[24] W. G. Harter and C. W. Patterson, J. Math. Phys. **20**, 1453 (1979).
[25] B. I. Zhilinskii and I. M. Pavlichenkov, Sov. Phys. JETP **65**, 221 (1887).
[26] I. M. Pavlichenkov and B. I. Zhilinskii, Ann. Phys. (Paris) **184**, 1 (1988).
[27] J. Makarewicz, Mol. Phys. **69**, 903 (1990); J. Chem. Phys. **108**, 469 (1998).
[28] S. V. Petrov and K. M. Katsov, Chem. Phys. Lett. **246**, 649 (1998).
[29] I. N. Kozin and R. M. Roberts (in preparation).
[30] B. T. Sutcliffe and J. Tennyson, Mol. Phys. **58**, 1053 (1986); Int. J. Quantum Chem. **39**, 183 (1991).
[31] J. K. G. Watson, Mol. Phys. **19**, 465 (1970).
[32] R. S. Mackay, in *Nonlinear Phenomena and Chaos*, edited by S. Sarkar (Adam Hilger, Bristol, 1986), pp. 254–270.
[33] P. R. Bunker, *Molecular Symmetry and Spectroscopy* (Academic, London, 1979).
[34] Note that here we do *not* follow Bunker (Ref. 33) who uses the notation $D_{\infty h}(M)$ for molecular symmetry group of symmetric linear molecule. $C_{2h}(M)$ is the subgroup of the extended $D_{\infty h}(EM)$ group which preserves the RE.
[35] J. C. van der Meer, *Lecture Notes in Mathematics* (Springer-Verlag, 1985), Vol 1160.
[36] S. L. Altman, *Induced Representations in Crystals and Molecules* (Academic, New York, 1977).
[37] E. P. Wigner, *Group Theory and Its Application to the Quantum Mechanics of Atomic Spectra* (Academic, London, 1968).
[38] J. J. Duistermaat, ZAMP **49**, 156 (1998).
[39] R. H. Cushman and J. J. Duistermaat, Bull. Am. Math. Soc. **19**, 475 (1988); M. S. Child, J. Phys. A **31**, 657 (1998); Vũ Ngọc San, Preprint 1055, University of Utrecht (1998); M. S. Child, T. Weston, and J. Tennyson, Mol. Phys. **96**, 371 (1999).
[40] W. A. Majewski, A. R. W. McKellar, D. Sadovskii, and J. K. G. Watson, Can. J. Phys. **72**, 1016 (1994).
[41] J. K. G. Watson, J. Mol. Spectrosc. **103**, 350 (1984).
[42] S. Carter and W. Meyer, J. Chem. Phys. **100**, 2104 (1994).
[43] O. L. Polyansky, J. Mol. Spectrosc. **112**, 79 (1985).
[44] J. K. G. Watson, S. C. Foster, A. R. W. McKellar, P. Bernath, T. Amano, F. S. Pan, M. W. Crofton, R. S. Altman, and T. Oka, Can. J. Phys. **62**, 1875 (1984).
[45] B. M. Dinelli, L. Neale, O. L. Polyansky, and J. Tennyson, J. Mol. Spectrosc. **181**, 142 (1997).
[46] S. Miller and J. Tennyson, Chem. Phys. Lett. **145**, 117 (1988).